Nat Biotechnol. Author manuscript; available in PMC 2016 September 20.

Published in final edited form as:

Nat Biotechnol. 2014 February ; 32(2): 182–190. doi:10.1038/nbt.2806.

Smac mimetics and innate immune stimuli synergize to promote tumor death

Shawn T. Beug[1], **Vera A. Tang**[1], **Eric C. LaCasse**[1], **Herman H. Cheung**[1], **Caroline E. Beauregard**[1], **Jan Brun**[1], **Jeffrey P. Nuyens**[1], **Nathalie Earl**[1], **Martine St-Jean**[1], **Janelle Holbrook**[1], **Himika Dastidar**[2], **Douglas J. Mahoney**[2], **Carolina Ilkow**[3], **Fabrice Le Boeuf**[3], **John C. Bell**[3,4], and **Robert G. Korneluk**[1,4,5]

[1]Solange Gauthier Karsh Molecular Genetics Laboratory, Apoptosis Research Centre, Children's Hospital of Eastern Ontario Research Institute, Ottawa, Ontario, Canada

[2]Alberta Children's Hospital Research Institute, Department of Microbiology, Immunology and Infectious Disease, University of Calgary, Calgary, Alberta, Canada

[3]Centre for Innovative Cancer Therapeutics, Ottawa Hospital Research Institute, Ottawa, Ontario, Canada

[4]Department of Biochemistry, Microbiology and Immunology, University of Ottawa, Ottawa, Ontario, Canada

Abstract

Smac mimetic compounds (SMC), a class of drugs that sensitize cells to apoptosis by counteracting the activity of inhibitor of apoptosis (IAP) proteins, have proven safe in Phase I clinical trials in cancer patients. However, because SMCs act by enabling transduction of pro-apoptotic signals, SMC monotherapy may only be efficacious in the subset of patients whose tumors produce large quantities of death-inducing proteins such as inflammatory cytokines. As such, we reasoned that SMCs would synergize with agents that stimulate a potent yet safe "cytokine storm". Here we show that oncolytic viruses and adjuvants such as poly(I:C) and CpG induce bystander death of cancer cells treated with SMCs that is mediated by interferon beta (IFNβ), tumor necrosis factor alpha (TNFα) and/or TNF-related apoptosis-inducing ligand (TRAIL). This combinatorial treatment resulted in tumor regression and extended survival in two mouse models of cancer. As these and other adjuvants have been proven safe in clinical trials, it may be worthwhile to explore their clinical efficacy in combination with SMCs.

[5]Corresponding author: Korneluk, R.G. bob@arc.cheo.ca.

AUTHOR CONTRIBUTIONS

S.T.B, E.C.L., V.A.T., F.L., D.J.M. and R.G.K designed the experiments. S.T.B., H.C.C., J.P.N., N.E., M.S.J., J.H., C.E.B., V.A.T, F.L., C.I., H.D. and J.B. conducted experiments. S.T.B., E.C.L., V.A.T., J.C.B. D.J.M. and R.G.K. wrote the manuscript.

COMPETING FINANCIAL INTERESTS

RGK is a scientific founder and shareholder of Aegera Therapeutics (Pharmascience Inc., Montreal, Canada) which has a SMC under clinical development. JCB is the Chief Scientific Officer and a shareholder of Jennerex (Ottawa, Canada and San Francisco, USA), which has a Vaccinia-based oncolytic virus under clinical development.

INTRODUCTION

Several Smac mimetic compounds (SMCs) are being evaluated in early- to mid-stage clinical trials in cancer patients[1]. SMCs are rationally designed based on the properties of Smac, an endogenous pro-apoptotic protein that, upon release from the mitochondria, binds to and antagonizes several members of the inhibitor of apoptosis (IAP) family. The IAP proteins are attractive cancer therapy targets because they regulate programmed cell death in tumour cells[1]. For example, the prototypical X-linked IAP (XIAP) protein, which directly inhibits key initiator and executioner caspase proteins within every programmed cell death cascade and can thereby thwart the completion of all cell death programs, is hyper-active in many human cancers[1,2]. In addition, genetic loss of the cellular IAP proteins 1 and 2 (cIAP1 and 2), which are E3 ubiquitin ligases that primarily regulate programmed cell death signalling pathways engaged by immune cytokines[3,4,5,6,7,8,9], causes tumor necrosis factor alpha (TNFα), TNF-related apoptosis-inducing ligand (TRAIL) and interleukin 1 beta (IL1β) to become toxic to the majority of cancer cells[5,6,7,8,9,10,11,12,13,14,15,16].

An important property of SMCs is that they target several IAPs, including XIAP and the cIAPs; as such, SMC therapy intervenes at multiple distinct yet interrelated stages of programmed cell death inhibition. This characteristic imbues two noteworthy advantages over most other molecularly targeted drugs: fewer opportunities for tumors to develop resistance, and more opportunities for synergy with existing and emerging cancer therapeutics, many of which activate pro-apoptotic pathways influenced by SMCs. For example, death-inducing inflammatory cytokines such as TNFα and IL-1β and pro-apoptotic proteins such as TRAIL potently synergize with SMC therapy in many tumour-derived cell lines in vitro. Therapeutic strategies aimed at increasing the abundance of these pro-apoptotic proteins in SMC-treated tumours, in particular using approaches that would limit the toxicities commonly associated with recombinant cytokine therapy, are thus very attractive.

TNFα, TRAIL and dozens of other cytokines and chemokines are upregulated in response to pathogen recognition by the innate immune system[17,18,19]. Importantly, this ancient response to microbial invaders is usually self-limiting and safe, due to stringent negative regulation that limits the strength and duration of its activity. We thus asked whether stimulating the innate immune system using pathogen mimetics would be a safe and effective strategy to generate a cytokine milieu sufficient to initiate programmed cell death in tumours treated with a SMC. We report here that non-pathogenic oncolytic viruses, as well as mimetics of microbial RNA or DNA (poly (I:C) and CpG, respectively) induce bystander killing of cancer cells treated with a SMC and that this death depends on interferon beta (IFNβ), TNFα and/or TRAIL production. Importantly, this combinatorial therapeutic strategy was tolerable *in vivo* in mice and led to durable cures in several mouse models of aggressive cancer.

RESULTS

Synergistic induction of bystander cell death

Oncolytic viruses are currently in phase I–III clinical evaluation in cancer patients[20]. A major barrier to effective oncolytic virus therapy is virus-induced expression of type I IFN and nuclear factor kappa b (NF-κB)-responsive cytokines, which orchestrate an antiviral state in tumours. We sought to exploit these cytokines to induce programmed cell death in cancer cells that were pretreated with a SMC. To begin, we screened a small panel of tumour-derived human and mouse (n=28) and normal (n=2) cell lines for responsiveness to the SMC LCL161 and the oncolytic rhabdovirus VSVΔ51. We chose LCL161 because this compound is the most clinically advanced drug in the SMC class[21,22,23] and VSVΔ51 because it is known to induce a robust antiviral cytokine response[24]. In 15 of the 28 tumor cell lines tested (54%), SMC treatment reduced the EC_{50} of VSVΔ51 by 10 – 10 000 fold (Supplementary Fig. 1, and representative examples in Fig. 1a–b). Similarly, low dose VSVΔ51 reduced the EC_{50} of SMC from undetermined levels (>2500 nM) to 4.5 and 21.9 nM in mouse mammary carcinoma EMT6 and human glioblastoma SNB75 cells, respectively (Fig. 1c). Combination index analyses determined that the interaction between SMC and VSVΔ51 was synergistic (Supplementary Fig. 2). Experiments using four other SMCs and five other oncolytic viruses showed that all tested monomer and dimer SMCs (containing one or two IAP binding motifs, respectively) synergize with VSVΔ51 in inducing EMT6 and SNB75 cell death (Supplementary Fig. 3). The oncolytic rhabdoviruses VSVΔ51 and Maraba-MG1 were superior in eliciting bystander killing in synergizing with SMCs compared to HSV, reovirus, vaccinia and wild-type VSV; this may be explained by the fact that the latter four viruses can use elaborate mechanisms to suppress innate immune signalling[20] (Supplementary Fig. 4). RNAi-mediated silencing of XIAP and the cIAPs demonstrated that synergy with VSVΔ51 required silencing of both XIAP and the cIAPs (Supplementary Fig. 5). In contrast to the results in tumour-derived cell lines, non-cancer GM38 primary human skin fibroblasts and human skeletal muscle myoblasts were unaffected by VSVΔ51 and SMC combination therapy (Supplementary Fig. 1). Taken together, these data indicate that oncolytic VSV synergizes with SMC therapy specifically in tumor cells.

To determine if VSVΔ51 elicits bystander cell death in neighboring uninfected cells, we treated cells with SMCs prior to infection with a low dose of VSVΔ51 (MOI = 0.01 infectious particles per cell). Immunofluorescent colocalization analyses revealed that the majority of uninfected EMT6 cells stained positive for cleaved caspase-3 (Fig. 1d), a marker of apoptosis; these findings suggest the induction of widespread bystander cell death. To complement this experiment, we assessed whether conditioned media derived from cells infected with VSVΔ51 (which was subsequently inactivated by UV light) could induce death when transferred to a plate of uninfected cancer cells treated with a SMC. The conditioned media induced cell death only when the cells were cotreated with a SMC (Fig. 1e). We also found that a low-dose of a pseudotyped G-less strain of VSVΔ51 (MOI = 0.1), containing a deletion of the gene encoding for its glycoprotein (VSVΔ51ΔG) that limits the virus to a single round of infection, was toxic to an entire plate of cancer cells treated with a SMC (Fig. 1f). Finally, we performed a cytotoxicity assay in cells overlaid with agarose, which

retards the spread of virus; we infected these cells with VSVΔ51 expressing a fluorescent tag[25,26], and observed death of SMC-treated cells outside of the zone of virus infection (Fig. 1g and Supplementary Fig. 6). Overall, these results indicate that VSVΔ51 infection leads to the release of at least one soluble factor that can potently induce bystander cell death in neighboring, uninfected cancer cells treated with SMCs.

SMCs do not suppress antiviral immunity

Mammalian cells respond to infection with an RNA virus through a signaling cascade initiated by members of a family of cytosolic (RIG-I-like receptors, RLRs) and endosomal (toll-like receptors, TLRs) viral RNA sensors[27]. Once triggered, these receptors activate IFN-response factor (IRF) 3/7 and NF-κB, which result in production of IFNs and IFN-responsive genes as well as an array of inflammatory chemokines and cytokines. This response 'warns' neighboring cells of an impending virus encounter, prompting those cells to pre-emptively express antiviral genes; it also promotes recruitment and activation of immune cells with the ability to clear the virus infection. Because the cIAP proteins were recently implicated in innate immune signalling pathways including those emanating from RLRs and TLRs[6,8], we asked whether SMC therapy alters the antiviral response to oncolytic VSV infection in tumor cells and in mice.

First, we evaluated the effect of SMC therapy on VSVΔ51 replication and spread. Single-step and multi-step virus growth curves revealed that SMC treatment does not affect the kinetics of VSVΔ51 growth in EMT6 or SNB75 cells *in vitro* (Fig. 2a). Similarly, time-lapse microscopy demonstrated that SMC treatment does not alter VSVΔ51 infectivity in or spread through tumor cells *in vitro* (Fig. 2b). We analyzed viral replication and spread *in vivo* by determining abundance of virus within tumor and normal tissue using an *in vivo* imaging system (IVIS) and tissue virus titration. We found no differences in the kinetics of viral spread in vehicle- or SMC-treated EMT6 tumor-bearing mice (Supplementary Fig. 7). These data provide indirect evidence that SMC treatment does not markedly affect the antiviral response of cancer and normal cells.

To directly analyze the antiviral response we measured IFNβ production in EMT6 and SNB75 cells treated with VSVΔ51 and SMCs. SMC-treated cancer cells responded to VSVΔ51 by secreting IFNβ (Fig. 2c), although in slightly lower amounts than vehicle-treated cancer cells. However, quantitative RT-PCR analysis of a small panel of IFN stimulated genes (ISGs) in cells treated with VSVΔ51 and vehicle or SMC revealed that SMC treatment did not markedly affect ISG gene expression (Fig. 2d). Consistent with this finding, Western blot analyses indicated that SMC treatment did not alter IFNβ-induced STAT1 phosphorylation (Fig. 2e). Finally, an IFN bioassay was used to measure the extent of protection of cells against cytopathic wild-type VSV. Supernatants obtained from EMT6 cells that were pretreated with SMC and VSVΔ51 provided protection against virus-induced cell death (Fig. 2f), thus demonstrating that SMC therapy does not alter the capacity of tumor cells to generate an antiviral response upon VSVΔ51 infection. Collectively, these data demonstrate that SMCs do not impede the ability of tumor cells to sense and respond to infection with VSVΔ51.

Mechanisms of bystander cell death

We previously showed that SMCs sensitize a number of cancer cell lines towards caspase-8-dependant apoptosis induced by TNFα, TRAIL and IL-1β[15,16]. As RNA viruses trigger the production of these cytokines, we investigated the involvement of cytokine signalling in death induced by combinatorial treatment with SMC and oncolytic virus. First, we treated cells with siRNA specific for the TNF receptor TNF-R1 and/or the TRAIL receptor DR5. This experiment revealed that TNFα and TRAIL are indispensable for bystander cell death induced by SMC and VSVΔ51 (Fig. 3 and Supplementary Fig. 8a). Western blot and immunofluorescence experiments revealed strong activation of the extrinsic apoptosis pathway; consistent with this, RNAi knockdown of caspase-8 and Rip1 revealed roles for these proteins in the bystander cell death induced by SMC and VSVΔ51 (Supplementary Fig. 9). Further solidifying a role for TNFα, engineering VSVΔ51 to express TNFα boosted cell death by an order of magnitude (Supplementary Fig. 10).

Next we silenced the type I IFN receptor (IFNAR1) and found, quite unexpectedly, that IFNAR1 knockdown prevented the synergy between SMC therapy and oncolytic VSV (Fig. 3b and Supplementary Fig. 8b). We predicted that IFNAR1 knockdown would dampen bystander killing, as TRAIL is a well-established ISG downstream of type I IFN signaling[28]. However, as TNFα and IL-1β are considered to be independent of IFN signalling (although responsive to NF-κB signalling downstream of virus detection) we predicted that IFNAR1 knockdown would not completely suppress bystander killing[29]. This result suggests the possibility of a non-canonical type I IFN-dependent pathway regulating the production of TNFα and/or IL-1β. Indeed, when we measured expression of transcripts encoding IFNβ, TRAIL, TNFα and IL-1β during an oncolytic VSV infection, we found a significant temporal lag between the induction of IFNβ and that of both TRAIL and TNFα (Fig. 3c). This data also suggests that TNFα – like TRAIL – may be induced secondary to IFNβ. To test this hypothesis, we treated cells with IFNAR1 siRNA before treating them with VSVΔ51. IFNAR1 knockdown completely abrogated the VSVΔ51-induced expression of both TRAIL and TNFα (Fig. 3d). Moreover, recombinant type I (IFNα/β) or type II IFN (IFNγ), but not type III IFN (IL28/29), effectively substituted for VSVΔ51 in synergizing with SMC to induce bystander killing (Fig. 3e).

To further explore this non-canonical pathway leading to induction of TNFα and TRAIL, we measured TRAIL and TNFα mRNA expression in SNB75 cells treated with recombinant IFNβ. Both cytokines were induced by IFNβ treatment (Fig. 3f) and ELISA experiments confirmed the production of their respective protein products in the cell culture media (Fig. 3g). Interestingly, there was a significant time lag between the induction of TRAIL and that of TNFα. As TRAIL is a *bona fide* ISG and TNFα is not, this result raised the possibility that TNFα is not induced by IFNβ directly, but responds to a downstream ISG up-regulated by IFNβ. We thus performed semi-quantitative RT-PCR on 176 putative ISGs in SNB75 cells and identified 70 that were significantly up-regulated by IFNβ (Supplementary Table 1). The potential roles of these ISGs in the induction of TNFα by IFNβ are currently being investigated. Notably, SMC treatment potentiated the induction of both TRAIL and TNFα by IFNβ in SNB75 cells (Fig. 3f–g). For example, in EMT6 cells, SMC treatment enhanced VSV-induced TNFα production by 5- to 7-fold (Supplementary Fig. 11). Furthermore, using

a dominant-negative construct of IKK we found that the production of these inflammatory cytokines downstream of IFNβ was dependent, at least in part, on classical NF-κB signalling (Fig. 3h). Finally, blocking TNF-R1 signalling (with antibodies or siRNA) prevented EMT6 cell death in the presence of SMC and VSVΔ51 or IFNβ (Supplementary Fig. 12).

In vivo synergistic effects

To evaluate SMC and oncolytic VSV co-therapy *in vivo*, we first used the EMT6 mammary carcinoma as a syngeneic, orthotopic model. Preliminary safety and pharmacodynamic experiments revealed that a dose of 50 mg/kg LCL161 delivered by oral gavage was well tolerated (transient loss of ~5% body weight that recovers within 5 d) and induced cIAP1/2 knockdown in tumours for at least 24 hrs, and up to 48–72 hours in some cases. The reduction in XIAP levels were not as pronounced (Supplementary Fig. 13). When tumours reached ~100 mm^3, we began treating mice twice weekly with vehicle or 50 mg/kg LCL161 (oral) and/or 5×10^8 PFU VSVΔ51 (i.v.). LCL161 therapy alone decreased the rate of tumour growth and modestly extended survival, whereas VSVΔ51 alone did not markedly alter tumour growth or mouse survival (Fig. 4a–b). However, combined SMC and VSVΔ51 treatment induced tumour regression and led to durable cures in 40% of the treated mice. Consistent with the bystander killing mechanism elucidated *in vitro*, immunofluorescence analyses revealed that the infectivity of VSVΔ51 was transient and limited to small foci within the tumour (Fig. 4c), whereas caspase-3 activation was widespread in the SMC and VSVΔ51 cotreated tumours (Fig. 4d). Furthermore, Western blots of tumour lysates demonstrated activation of caspase-8 and -3 in doubly-treated tumours (Fig. 4e). While the animals in the combination treatment cohort experienced weight loss, the mice fully recovered following the last treatment (Supplementary Fig. 14a).

To confirm these *in vivo* data in another model system, we tested the human HT-29 colorectal adenocarcinoma xenograft model in nude (athymic) mice. HT-29 is a cell line that is highly responsive to bystander killing by SMC and VSVΔ51 co-treatment *in vitro* (Supplementary Fig. 15a, b). Similar to our findings in the EMT6 model system, combination therapy with 50 mg/kg LCL161 (oral) and 1×10^8 PFU (intratumoral) of VSVΔ51 slowed tumour growth and lead to a significant extension of mouse survival (Supplementary Fig. 15c). In contrast, neither monotherapy had any effect on HT-29 tumours. Furthermore, there was no additional weight loss in the double treated mice compared to SMC treated mice (Supplementary Fig. 15d). These results in the HT-29 model indicate that the synergy between SMC and VSVΔ51 does not completely require the adaptive immune response.

Next, we wished to determine whether oncolytic virus infection coupled with SMC treatment leads to TNFα- and/or IFNβ-mediated cell death *in vivo*. Compared to an isotype control antibody, TNFα neutralizing antibody prevented SMC and VSVΔ51-induced EMT6 tumour regression and mouse survival extension (Fig. 4f, g). However, treatment of Balb/c mice bearing EMT6 tumours with IFNAR1 blocking antibodies resulted in mouse death due to viremia within 24–48 hrs post infection. Nevertheless, prior to mouse death and 18–20 hrs after virus infection, we collected tumors and analyzed caspase activity. Compared to SMC and VSVΔ51-treated mice injected with isotype control antibody, those injected with anti-

IFNAR1 showed no caspase-8 activity and much less caspase-3 activity (Supplementary Fig. 16). These results support the hypothesis that intact TNFα and type I IFN signalling is required to mediate the *in vivo* anti-tumour effects of the combinatorial treatment.

To assess the contribution of innate immune cells or other immune mediators to the efficacy of combination therapy, we first attempted to treat EMT6 tumours in immunodeficient NOD-scid or NSG (NOD-scid-IL2Rgamma^{null}) mice. However, similar to mice treated with anti-IFNAR1, these mice died rapidly due to viremia (data not shown). Therefore, we addressed the contribution of innate immune cells in an *ex vivo* splenocyte culture system. Sorted splenic macrophages (CD11b$^+$ F4/80$^+$), neutrophils (CD11b$^+$ Gr1$^+$), NK cells (CD11b$^-$ CD49b$^+$) and non-myeloid (CD11b$^-$ CD49$^-$) populations were stimulated with VSVΔ51, and the conditioned medium was transferred to EMT6 cells treated with SMC or vehicle. VSVΔ51-stimulated macrophages and neutrophils, but not NK cells, are capable of producing factors that lead to cancer cell death in the presence of SMCs (Supplementary Fig. 17a). We also isolated primary macrophages from bone marrow and these macrophages also responded to oncolytic VSV infection in a dose-dependent manner to produce factors which kill EMT6 cells (Supplementary Fig. 17b). Altogether, these findings demonstrate that multiple innate immune cell populations can mediate the observed anti-tumour effects, but that macrophages may be the most likely effectors of this response.

Adjuvants potentiate SMC effects *in vivo*

We next investigated whether synthetic TLR agonists (often used as adjuvants) known to induce an innate proinflammatory response, could replace oncolytic virus and synergize with SMCs. We co-cultured EMT6 cells with mouse splenocytes in a transwell insert system, and treated the splenocytes with SMC and agonists of TLR 3, 4, 7 or 9. All of the tested TLR agonists induced the bystander death of SMC treated EMT6 cells (Fig. 5a). The TLR4, 7 and 9 agonists LPS, imiquimod and CpG, respectively, required splenocytes to induce bystander killing of EMT6 cells, presumably because their target TLR receptors are not expressed in EMT6 cells. However, the TLR3 agonist poly(I:C) lead to EMT6 cell death in the absence of splenocytes.

We next tested poly(I:C) and CpG in combination with SMC therapy *in vivo*. We chose these adjuvants as they have proven to be safe in humans and are currently being evaluated in numerous mid to late stage clinical trials for cancer[32,33,34,35]. EMT6 tumours were established and treated as described above. While poly(I:C) treatment had no bearing on tumour growth as a single agent, when combined with SMCs it induced substantial tumor regression and, when delivered intraperitoneally, led to durable cures in 60% of the treated mice (Fig. 5b–c). Similarly, CpG monotherapy had no bearing on tumour size or survival, but when combined with SMC therapy led to tumour regressions and durable cures in 88% of the treated mice (Fig. 5d–e). Markedly, the most effective therapy was with the combination of SMC with local (intratumoral) and systemic (i.v.) administration of CpG, presumably because of the increased concentration of proinflammatory cytokines within the tumor milieu. Importantly, these combination therapies were well tolerated by the mice, and their body weight returned to pre-treatment levels shortly after the cessation of therapy

(Supplementary Fig. 14b, c). Together these data demonstrate that a series of clinically advanced innate immune adjuvants strongly and safely synergize with SMC therapy *in vivo*.

DISCUSSION

SMC medicines are rapidly progressing through clinical evaluation, however, SMCs will likely require rationally-designed therapeutic partners to be maximally effective[1]. Here we demonstrate a new strategy for boosting the efficacy of SMC therapy, specifically the stimulation of a host innate immune response. Our approach is broadly useful in that it works with different SMCs and a number of pathogen-mimetics in a large percentage of examined tumor cell lines. In addition, this combinatorial approach was efficacious in various aggressive, treatment refractory murine tumour models. Several of the SMCs studied here are in early-mid stage clinical evaluation and all of the pathogen-mimetics/adjuvants examined here are currently in phase I–III clinical trials[23,32,33,34,35,36,37]. Data from the human studies has indicated that each of these medicines is safe[23,36,37], but none appear to be particularly effective as monotherapies. Our strategy overcomes the limitations of both Smac- and pathogen-mimetics as single agents, at least in cell-based and murine model systems.

Type I and II IFNs, including the therapeutically relevant cytokines IFNα and IFNβ, were effectors of SMC-induced tumour killing. This unexpected discovery will ultimately shed light on IFN biology and death pathways involving caspase-8, which are controlled by the cIAPs and XIAP, and which can now be further explored and exploited therapeutically in combination with SMCs. The relationship between type I IFN and TNFα is complex, as these two cytokines have complimentary or opposing effects depending on the biological context[30,31]. However, in the context of SMC plus oncolytic virus treatment, a simple working model can be proposed (Supplementary Fig. 18). Tumor cells infected by an oncolytic RNA virus up-regulate type I IFN, and this process is not affected by SMC antagonism of the IAP proteins. Those IFNs in turn signal to the same cancer cell (autocrine) and neighboring uninfected cancer cells (paracrine) and induce secretion of TNFα and TRAIL; this process is enhanced by SMC treatment. In the presence of SMC and the cytokines TNFα and/or TRAIL, bystander tumor cells undergo caspase-8 dependent apoptosis.

Previous work indicated that a SMC can enhance the adaptive immune response against a B16 melanoma tumour by boosting cancer vaccine-induced T-cell activity[3,4]. In contrast, our findings underscore the critical role that the innate immune response plays in this combination approach. Furthermore, while many other approaches to improve SMC therapy have been attempted, very rarely have complete responses been observed, particularly in aggressive tumors in immunocompetent mice. The one exception was co-treatment with SMC and recombinant TRAIL, which led to durable cures in at least one mouse model system[38]. We suspect that using a pathogen-mimetic, whose mechanism of action is partially dependent on TRAIL, is a superior approach for two reasons. First, this approach also induces TNFα-mediated apoptosis and necroptosis, and given the plasticity and heterogeneity of most advanced cancers, simultaneously inducing multiple distinct cell death mechanisms is more likely to be effective for treating these diseases and is less likely to

develop resistance to treatment. Second, pathogen-mimetics elicit an integrated innate immune response that includes layers of negative feedback. We suspect that these feedback mechanisms act to temper the cytokine response in ways that are difficult to replicate using recombinant proteins, and thus act as a safeguard to prevent toxicity of this combination therapy.

METHODS

Reagents

Novartis provided LCL161[21,22]. SM-122 and SM-164 were provided by Dr. Shaomeng Wang (University of Michigan, USA)[39]. AEG40730[40] was synthesized by Vibrant Pharma Inc. OICR720 was synthesized by the Ontario Institute for Cancer Research (OICR)[41]. IFNα, IFNβ, IL28 and IL29 were obtained from PBL Interferonsource. All siRNAs were obtained from Dharmacon (ON-TARGETplus SMARTpool). CpG-ODN 2216 was synthesized by IDT (5′-gggGGACGATCGTCgggggg-3′, lowercase indicates phosphorothioate linkages between these nucleotides, while underlining identifies three CpG motifs with phosphodiester linkages). Imiquimod was purchased from BioVision Inc. poly(I:C) was obtained from Invivogen. LPS was from Sigma.

Cell culture

Cells were maintained at 37°C and 5% CO_2 in DMEM media supplemented with 10% heat-inactivated fetal calf serum, penicillin, streptomycin and 1% non-essential amino acids (Invitrogen). All of the cell lines were obtained from ATCC, with the following exceptions: SNB75 (Dr. D. Stojdl, Children's Hospital of Eastern Ontario Research Institute) and SF539 (UCSF Brain Tumour Bank). Cell lines were regularly tested for mycoplasma contamination. For siRNA transfections, cells were reverse transfected with Lipofectamine RNAiMAX (Invitrogen) or DharmaFECT I (Dharmacon) for 48 hr as per the manufacturer's protocol.

Viruses

The Indiana serotype of VSVΔ51[42] was used in this study and was propagated in Vero cells. VSVΔ51-GFP is a recombinant derivative of VSVΔ51 expressing jelly fish green fluorescent protein. VSVΔ51–Fluc expresses firefly luciferase. VSVΔ51 with the deletion of the gene encoding for glycoprotein (VSVΔ51ΔG) was propagated in HEK293T cells that were transfected with pMD2-G using Lipofectamine2000 (Invitrogen). To generate the VSVΔ51-TNFα construct, full-length mouse TNFα gene was inserted between the G and L viral genes. All VSVΔ51 viruses were purified on a sucrose cushion. Maraba-MG1, VVDD-B18R^{-}, Reovirus and HSV1 ICP34.5 were generated as previously described[43,44,45]. Generation of adenoviral vectors expressing GFP or coexpressing GFP and dominant negative IKKβ was as previously described[16].

In vitro viability assay

Cell lines were seeded in 96-well plates and incubated overnight. Cells were treated with vehicle (0.05% DMSO) or 5 μM LCL161 and infected with the indicated MOI of oncolytic virus or treated with 250 U/mL IFNβ, 500 U/mL IFNα, 500 U/mL IFNγ, 10 ng/mL IL28 or

10 ng/mL IL29 for 48 hours. Cell viability was determined by Alamar blue (Resazurin sodium salt (Sigma))[46] and data were normalized to vehicle treatment. The chosen sample size is consistent with previous reports that used similar analyses for viability assays, but no statistical methods were used to determine sample size[15,16]. For combination indices (CI), cells were seeded overnight, treated with serial dilutions of a fixed combination mixture of VSVΔ51 and LCL161 (5000:1, 1000:1 and 400:1 ratios of PFU VSVΔ51: μM LCL161) for 48 hours and cell viability was assessed by Alamar blue. CI were calculated according to the method of Chou and Talalay using Calcusyn[47]. An n = 3–4 of biological replicates was used to determine statistical measures (mean, standard deviation or standard error).

Spreading assay

A confluent monolayer of 786-0 cells was overlaid with 0.7% agarose in complete media. A small hole was made with a pipette in the agarose overlay in the middle of the well where 5×10^2 PFU of VSVΔ51-GFP was administered. Media containing vehicle or 5 μM LCL161 was added on top of the overlay, cells were incubated for 4 days, fluorescent images were acquired, and cells were stained with crystal violet. An n = 3 of biological replicates was used to determine statistical measures (mean, standard deviation)

Splenocyte coculture

EMT6 cells were cultured in multiwell plates and overlaid with cell culture transwell inserts containing unfractionated splenocytes. Single-cell splenocyte suspensions were obtained by passing mouse spleens through 70 μm nylon mesh and red blood cells were lysed with ACK lysis buffer. Splenocytes were co-treated for 24 hr with 1 μM LCL161 and 0.1 MOI of VSVΔ51ΔG, 1 ug/mL poly(I:C), 1 ug/mL LPS, 2 μM imiquimod or 0.25 μM CpG. EMT6 cell viability was determined by crystal violet staining. An n = 3 of biological replicates was used to determine statistical measures (mean, standard deviation).

Cytokine responsiveness bioassay

Cells were infected with the indicated MOI of VSVΔ51 for 24 hr and the cell culture supernatant was exposed to UV light for 1 hr to inactive VSVΔ51 particles. Subsequently, the UV-inactivated supernatant was applied to naive cells in the presence of 5 μM LCL161 for 48 hr. Cell viability was assessed by Alamar blue. An n = 3 of biological replicates was used to determine statistical measures (mean, standard deviation).

Microscopy

To determine the kinetics of VSVΔ51 spread, cells were infected with VSVΔ51-GFP and cells were placed in an incubator outfitted with an Incucyte Zoom microscope equipped with a 10X objective. Phase-contrast and fluorescence images of four fields per well were automatically acquired every 30 min over a span of 48 hr. To visualize bystander cell death via immunofluorescence, cells were treated with 5 μM LCL161 and 0.01 MOI of VSVΔ51-GFP for 36 hr and labelled with the Magic Red Caspase-3/7 Assay Kit (ImmunoChemsitry Technologies). Images were acquired on an InCell Analyzer 6000 (GE). To measure the proportion of caspase-3/7 activity, 5 μM LCL161, the indicated MOI of VSVΔ51 and 5 μM CellPlayer Apoptosis Caspase-3/7 reagent (Essen Bioscience) was added to the cells. Cells

were imaged with the Incucyte Zoom. To measure the proportion of apoptotic cells, 1 ug/mL Annexin V-CF594 (Biotium) and 0.2 μM YOYO-1 (Invitrogen) was added to SMC and VSVΔ51 treated cells at 24 hr post-treatment. Images were acquired using the IncuCyte Zoom. Enumeration of fluorescence signals from the Incucyte Zoom was processed using the integrated object counting algorithm within the IncuCyte Zoom software. An n = 12 (VSVΔ51-GFP), n = 12 (caspase-3/7) or n = 9 (Annexin V, YOYO-1) of biological replicates was used to determine statistical measures (mean, standard deviation).

Multiple step growth curves

Cells were treated with vehicle or 5 μM LCL161 for 2 hr and subsequently infected at the indicated MOI of VSVΔ51 for 1 hr. Cells were washed with PBS, and cells were replenished with media containing vehicle or 5 μM LCL161 and incubated at 37°C. Aliquots were obtained at the indicated times and viral titres assessed by a standard plaque assay using African green monkey VERO cells.

Western blotting

Cells were scraped, collected by centrifugation and lysed in RIPA lysis buffer containing a protease inhibitor cocktail (Roche). Equal amounts of soluble protein were separated on polyacrylamide gels followed by transfer to nitrocellulose membranes. Individual proteins were detected by Western blotting using the following antibodies: pSTAT1 (9171), caspase-3 (9661), caspase-8 (9746), caspase-9 (9508), DR5 (3696), TNF-R1 (3736), cFLIP (3210), and PARP (9541) from Cell Signalling Technology; caspase-8 (1612) from Enzo Life Sciences; IFNAR1 (EP899) and TNF-R1 (19139) from Abcam; caspase-8 (AHZ0502) from Invitrogen; cFLIP (clone NF6) from Alexis Biochemicals; RIP1 (clone 38) from BD Biosciences; and E7 from Developmental Studies Hybridoma Bank. Our rabbit anti-rat IAP1 and IAP3 polyclonal antibodies were used to detect human and mouse cIAP1/2 and XIAP, respectively[9]. AlexaFluor680 (Invitrogen) or IRDye800 (Li-Cor) were used to detect the primary antibodies, and infrared fluorescent signals were detected using the Odyssey Infrared Imaging System (Li-Cor). Full-length Western blots are presented in Supplementary Fig. 19.

RT-qPCR

Total RNA was isolated from cells using the RNAEasy Mini Plus kit (Qiagen). Two step RT-qPCR was performed using Superscript III (Invitrogen) and SsoAdvanced SYBR Green supermix (BioRad) on a Mastercycler ep realplex (Eppendorf). All primers were obtained from realtimeprimers.com (Supplementary Table 2). An n = 3 of biological replicates was used to determine statistical measures (mean, standard deviation).

ELISA

Cells were infected with virus at the indicated MOI or treated with IFNβ for 24 hours, cell culture debris was removed by centrifugation and cytokines within the supernatant was measured with the TNFα Quantikine high sensitivity, TNFα DuoSet, TRAIL DuoSet (R&D Systems) or VeriKine IFNβ (PBL Interferonsource) assay kits. In some cases, the cell

culture supernatants were concentrated using Amicon Ultra filtration units. An n = 3 of biological replicates was used to determine statistical analysis (mean, standard deviation).

EMT6 mammary tumour model

Mammary tumours were established by injecting 1×10^5 wild-type EMT6 or firefly luciferase-tagged EMT6 (EMT6-Fluc) cells in the mammary fat pad of 6-week old female BALB/c mice. Mice with palpable tumors (~100 mm^3) were cotreated with either vehicle (30% 0.1 M HCl, 70% 0.1 M NaOAc pH 4.63) or 50 mg/kg LCL161 orally and either i.v. injections of either PBS or 5×10^8 PFU of VSVΔ51 twice weekly for two weeks. For poly(I:C) and SMC treatments, animals were treated with LCL161 twice a week and either PBS (intratumoral (i.t.)), 20 ug poly(I:C) i.t. or 2.5 mg/kg poly(I:C) i.p. four times a week. The SMC and CpG group was injected with 2 mg/kg CpG (i.p.) and the next day was followed with CpG and SMC treatments. The CpG and SMC treatments were repeated 4 d later. Treatment groups were assigned by cages and each group had minimum 4–8 mice for statistical measures (mean, standard error; Kaplan-Meier with log rank analysis). The sample size is consistent with previous reports that examined tumour growth and mouse survival following cancer treatment but no statistical methods were used to determine sample size[26,43,44]. Blinding was not possible. Animals were euthanized when tumours metastasized intraperitoneally or when the tumour burden exceeded 2000 mm^3. Tumour volume was calculated using $(\pi)(W)^2(L)/4$ where W = tumour width and L = tumour length. Tumour bioluminescence imaging was captured with a Xenogen2000 IVIS CCDcamera system (Caliper Life Sciences) following i.p. injection of 4 mg luciferin (Gold Biotechnology).

HT-29 subcutaneous tumour model

Subcutaneous tumours were established by injecting 3×10^6 HT-29 cells in the right flank of 6-week old female CD-1 nude mice. Palpable tumours (~200 mm^3) were treated with five i.t. injections of PBS or 1×10^8 PFU of VSVΔ51. Four hours later, mice were administered vehicle or 50 mg/kg LCL161 orally. Treatment groups were assigned by cages and each group had a minimum of 5–7 mice for statistical measures (mean, standard error; Kaplan-Meier with log rank analysis). The sample size is consistent with previous reports that examined tumour growth and mouse survival following cancer treatment but no statistical measures were used to determine sample size[26,43,44]. Blinding was not possible. Animals were euthanized when tumour burden exceeded 2000 mm^3. Tumour volume was calculated using $(\pi)(W)^2(L)/4$ where W = tumour width and L = tumour length.

All animal experiments were conducted with the approval of the University of Ottawa Animal Care and Veterinary Service in concordance with guidelines established by the Canadian Council on Animal Care.

Antibody-mediated cytokine neutralization

For neutralizing TNFα signalling *in vitro*, 25 ug/mL of α-TNFα (XT3.11) or isotype control (HRPN) was added to EMT6 cells for 1 hr prior to LCL161 and VSVΔ51 or IFNβ co-treatment for 48 hr. Viability was assessed by Alamar blue. An n = 3 of biological replicates was used to determine statistical measures (mean, standard deviation). For

neutralizing TNFα in the EMT6-Fluc tumor model, 0.5 μg of TNFα or HRPN was administered i.p. 8, 10 and 12 days post-implantation. Mice were treated with 50 mg/kg LCL161 (oral) on 8, 10 and 12 days post-implantation and were infected with 5×10^8 PFU VSVΔ51 i.v. on days 9, 11 and 13. Treatment groups were assigned by cages and each group had minimum 4–8 mice for statistical measures (mean, standard error; Kaplan-Meier with log rank analysis). The sample size is consistent with previous reports that examined tumour growth and mouse survival following cancer treatment but no statistical methods were used to determine sample size[26,43,44]. Blinding was not possible. Animals were euthanized when tumours metastasized intraperitoneally or when the tumour burden exceeded 2000 mm^3. Tumour volume was calculated using $(\pi)(W)^2(L)/4$ where W = tumour width and L = tumour length. For neutralization of type I IFN signalling, 2.5 μg of IFNAR1 (MAR1-5A3) or isotype control (MOPC-21) were injected i.p. into EMT6-tumour bearing mice and treated with 50 mg/kg LCL161 (oral) for 20 hr. Mice were infected with 5×10^8 PFU VSVΔ51 (i.v.) for 18–20 hr and tumours were processed for Western blotting. All antibodies were from BioXCell.

Flow cytometry and sorting

EMT6 cells were cotreated with 0.1 MOI of VSVΔ51-GFP and 5 μM LCL161 for 20 hr. Cells were trypsinized, permeabilized with the CytoFix/CytoPerm kit (BD Biosciences) and stained with APC-TNFα (MP6-XT22, BD Biosciences). Cells were analyzed on a Cyan ADP 9 flow cytometer (Beckman Coulter) and data was analyzed with FlowJo (Tree Star).

Splenocytes were enriched for CD11b using the EasySep CD11b positive selection kit (StemCell Technologies). $CD49^+$ cells were enriched using the EasySep CD49b positive selection kit (StemCell Technologies) from the $CD11b^-$ fraction. $CD11b^+$ cells were stained with F4/80-PE-Cy5 (BM8, eBioscience) and Gr1-FITC (RB6-8C5, BD Biosciences) and further sorted with MoFlo Astrios (Beckman Coulter). Flow cytometry data was analyzed using Kaluza (Beckman Coulter). Isolated cells were infected with VSVΔ51 for 24 hr and clarified cell culture supernatants was applied to EMT6 cells for 24 hr in the presence of 5 μM LCL161. An n = 3 of biological replicates was used to determine statistical measures (mean, standard deviation).

Bone marrow derived macrophages

Mouse femurs and radius were removed and flushed to remove bone marrow. Bone marrow cells were cultured in petri dishes with RPMI, 8% FBS and 5 ng/ml of M-CSF for 7 days. Flow cytometry was used to confirm the purity of the adherent macrophages ($F4/80^+$ $CD11b^+$).

Immunohistochemistry

Excised tumours were fixed in 4% PFA, embedded in a 1:1 mixture of OCT compound and 30% sucrose, and sectioned on a cryostat at 12 μm. Sections were permeablized with 0.1% Triton X-100 in blocking solution (50 mM Tris–HCl pH 7.4, 100 mM L-lysine, 145 mM NaCl and 1% BSA, 10% goat serum). α-cleaved caspase 3 (C92-605, BD Pharmingen) and polyclonal antiserum VSV (Dr. Earl Brown, University of Ottawa, Canada) were incubated

overnight followed by secondary incubation with AlexaFluor-coupled secondary antibodies (Invitrogen).

Statistical analysis

Comparison of Kaplan-Meier survival plots was conducted by log-rank analysis and subsequent pairwise multiple comparisons were performed using the Holm-Sidak method (SigmaPlot). Calculation of EC_{50} values was performed in GraphPad Prism using normalized nonlinear regression analysis (variable slope). The EC_{50} shift was calculated by subtracting the $\log_{10}$ EC_{50} of SMC-treated and VSVΔ51-infected cells from $\log_{10}$ EC_{50} of vehicle treated cells infected by VSVΔ51. To normalize the degree of SMC synergy, the EC_{50} value was scaled to 100% to compensate for cell death induced by SMC treatment alone.

Supplementary Material

Refer to Web version on PubMed Central for supplementary material.

Acknowledgments

We thank Drs. Dale Porter, Brant Firestone, Leigh Zawel, and J. Scott Cameron of Novartis for providing LCL161. SM-164 and SM-122 were kindly provided by Dr. Shaomeng Wang (University of Michigan, USA). We thank Dr. Rima Al-awar and her medicinal chemistry team at the Ontario Institute for Cancer Research (OICR) for providing OICR720. We thank Stephanie Pichette for her assistance with the creation of VSVΔ51-TNFα. This work is supported by grants awarded to RGK by the Canadian Institutes of Health Research (CIHR), the Ottawa Regional Cancer Foundation (ORCF), the Ottawa Kiwanis Medical Foundation, the Children's Hospital of Eastern Ontario (CHEO) Foundation, and The Lotte & John Hecht Memorial Foundation Innovation Grant of the Canadian Cancer Society. JCB is supported by OICR and The Terry Fox Foundation. FLB was supported by an industrial fellowship from CIHR. DJM is the recipient of a New Investigator Award from the Alliance for Cancer Gene Therapy (USA). RGK is a Fellow of the Royal Society of Canada and a Distinguished Professor of the University of Ottawa.

References

1. Fulda S, Vucic D. Targeting IAP proteins for therapeutic intervention in cancer. Nature Rev Drug Discov. 2012; 11:109–124. [PubMed: 22293567]
2. LaCasse EC. Pulling the plug on a cancer cell by eliminating XIAP with AEG35156. Cancer Lett. 2013; 332:215–224. [PubMed: 22776562]
3. Dougan M, et al. IAP inhibitors enhance co-stimulation to promote tumour immunity. J Exp Med. 2010; 207:2195–2206. [PubMed: 20837698]
4. Vanneman M, Dranoff G. Combining immunotherapy and targeted therapies in cancer treatment. Nat Rev Cancer. 2012; 12:237–251. [PubMed: 22437869]
5. Gyrd-Hansen M, Meier P. IAPs: from caspase inhibitors to modulators of NF-kappaB, inflammation and cancer. Nat Rev Cancer. 2010; 10:561–574. [PubMed: 20651737]
6. Vandenabeele P, Bertrand MJ. The role of the IAP E3 ubiquitin ligases in regulating pattern-recognition receptor signalling. Nat Rev Immunol. 2012; 12:833–844. [PubMed: 23124073]
7. Varfolomeev E, et al. Cellular inhibitors of apoptosis are global regulators of NF-kappaB and MAPK activation by members of the TNF family of receptors. Sci Signal. 2012; 5:ra22. [PubMed: 22434933]
8. Beug ST, Cheung HH, LaCasse EC, Korneluk RG. Modulation of immune signalling by inhibitors of apoptosis. Trends Immunol. 2012; 33:535–545. [PubMed: 22836014]
9. Mahoney DJ, et al. Both cIAP1 and cIAP2 regulate TNFalpha-mediated NF-kappaB activation. Proc Natl Acad Sci U S A. 2008; 105:11778–11783. [PubMed: 18697935]

10. Li L, et al. A Small Molecule Smac Mimic Potentiates TRAIL- and TNF{alpha}-Mediated Cell Death. Science. 2004; 305:1471–1474. [PubMed: 15353805]
11. Varfolomeev E, et al. IAP antagonists induce autoubiquitination of c-IAPs, NF-kappaB activation, and TNFalpha-dependent apoptosis. Cell. 2007; 131:669–681. [PubMed: 18022362]
12. Vince JE, et al. IAP antagonists target cIAP1 to induce TNFalpha-dependent apoptosis. Cell. 2007; 131:682–693. [PubMed: 18022363]
13. Petersen SL, et al. Autocrine TNFalpha signalling renders human cancer cells susceptible to Smac-mimetic-induced apoptosis. Cancer Cell. 2007; 12:445–456. [PubMed: 17996648]
14. Gaither A, et al. A Smac mimetic rescue screen reveals roles for inhibitor of apoptosis proteins in tumour necrosis factor-alpha signalling. Cancer Res. 2007; 67:11493–11498. [PubMed: 18089776]
15. Cheung HH, Mahoney DJ, Lacasse EC, Korneluk RG. Down-regulation of c-FLIP Enhances death of cancer cells by smac mimetic compound. Cancer Res. 2009; 69:7729–7738. [PubMed: 19773432]
16. Cheung HH, et al. Smac mimetic compounds potentiate interleukin-1 beta-mediated cell death. J Biol Chem. 2010:40612–40623. [PubMed: 20956527]
17. Kawai T, Akira S. The role of pattern-recognition receptors in innate immunity: update on Toll-like receptors. Nat Immunol. 2010; 11:373–384. [PubMed: 20404851]
18. Chen G, Shaw MH, Kim YG, Nunez G. NOD-like receptors: role in innate immunity and inflammatory disease. Annu Rev Pathol. 2009; 4:365–398. [PubMed: 18928408]
19. McFadden G, Mohamed MR, Rahman MM, Bartee E. Cytokine determinants of viral tropism. Nat Rev Immunol. 2009; 9:645–655. [PubMed: 19696766]
20. Russell SJ, Peng KW, Bell JC. Oncolytic virotherapy. Nat Biotechnol. 2012; 30:658–670. [PubMed: 22781695]
21. Houghton PJ, et al. Initial testing (stage 1) of LCL161, a SMAC mimetic, by the Pediatric Preclinical Testing Program. Pediatr Blood Cancer. 2012; 58:636–639. [PubMed: 21681929]
22. Chen KF, et al. Inhibition of Bcl-2 improves effect of LCL161, a SMAC mimetic, in hepatocellular carcinoma cells. Biochemical Pharmacology. 2012; 84:268–277. [PubMed: 22580047]
23. Dhuria S, et al. Time-Dependent Inhibition and Induction of Human Cytochrome P4503A4/5 by an Oral IAP Antagonist, LCL161, In Vitro and In Vivo in Healthy Subjects. J Clin Pharmacol. 2013; 53:642–653. [PubMed: 23585187]
24. Breitbach CJ, et al. Targeted inflammation during oncolytic virus therapy severely compromises tumour blood flow. Mol Ther. 2007; 15:1686–1693. [PubMed: 17579581]
25. Vaha-Koskela MJ, et al. Resistance to two heterologous neurotropic oncolytic viruses, Semliki Forest virus and vaccinia virus, in experimental glioma. J Virol. 2013; 87:2363–2366. [PubMed: 23221568]
26. Le Boeuf F, et al. Model-based rational design of an oncolytic virus with improved therapeutic potential. Nat Commun. 2013; 4:1974. [PubMed: 23764612]
27. Kawai T, Akira S. Innate immune recognition of viral infection. Nat Immunol. 2006; 7:131–137. [PubMed: 16424890]
28. Kirshner JR, Karpova AY, Kops M, Howley PM. Identification of TRAIL as an interferon regulatory factor 3 transcriptional target. J Virol. 2005; 79:9320–9324. [PubMed: 15994827]
29. Bose S, Kar N, Maitra R, DiDonato JA, Banerjee AK. Temporal activation of NF-kappaB regulates an interferon-independent innate antiviral response against cytoplasmic RNA viruses. Proc Natl Acad Sci U S A. 2003; 100:10890–10895. [PubMed: 12960395]
30. Cantaert T, Baeten D, Tak PP, van Baarsen LG. Type I IFN and TNFalpha cross-regulation in immune-mediated inflammatory disease: basic concepts and clinical relevance. Arthritis Res Ther. 2010; 12:219. [PubMed: 21062511]
31. Yarilina A, Ivashkiv LB. Type I interferon: a new player in TNF signalling. Curr Dir Autoimmun. 2010; 11:94–104. [PubMed: 20173389]
32. Rosenfeld MR, et al. A multi-institution phase II study of poly-ICLC and radiotherapy with concurrent and adjuvant temozolomide in adults with newly diagnosed glioblastoma. Neuro Oncol. 2010; 12:1071–1077. [PubMed: 20615924]

33. Butowski N, et al. A phase II clinical trial of poly-ICLC with radiation for adult patients with newly diagnosed supratentorial glioblastoma: a North American Brain Tumour Consortium (NABTC01–05). J Neurooncol. 2009; 91:175–182. [PubMed: 18797818]
34. Butowski N, et al. A North American brain tumour consortium phase II study of poly-ICLC for adult patients with recurrent anaplastic gliomas. J Neurooncol. 2009; 91:183–189. [PubMed: 18850068]
35. Krieg AM. CpG still rocks! Update on an accidental drug. Nucleic Acid Ther. 2012; 22:77–89. [PubMed: 22352814]
36. Erickson RI, et al. Toxicity profile of small-molecule IAP antagonist GDC-0152 is linked to TNF-alpha pharmacology. Toxicol Sci. 2013; 131:247–258. [PubMed: 22956632]
37. Wong H, et al. Dogs are more sensitive to antagonists of inhibitor of apoptosis proteins than rats and humans: a translational toxicokinetic/toxicodynamic analysis. Toxicol Sci. 2012; 130:205–213. [PubMed: 22843607]
38. Lu JF, et al. Therapeutic Potential and Molecular Mechanism of a Novel, Potent, Nonpeptide, Smac Mimetic SM-164 in Combination with TRAIL for Cancer Treatment. Molecular Cancer Therapeutics. 2011; 10:902–914. [PubMed: 21372226]
39. Sun H, et al. Design, synthesis, and characterization of a potent, nonpeptide, cell-permeable, bivalent Smac mimetic that concurrently targets both the BIR2 and BIR3 domains in XIAP. J Am Chem Soc. 2007; 129:15279–15294. [PubMed: 17999504]
40. Bertrand MJ, et al. cIAP1 and cIAP2 facilitate cancer cell survival by functioning as E3 ligases that promote RIP1 ubiquitination. Mol Cell. 2008; 30:689–700. [PubMed: 18570872]
41. Enwere EK, et al. TWEAK and cIAP1 regulate myoblast fusion through the noncanonical NF-kappaB signalling pathway. Sci Signal. 2013; 5:ra75.
42. Stojdl DF, et al. VSV strains with defects in their ability to shutdown innate immunity are potent systemic anti-cancer agents. Cancer Cell. 2003; 4:263–275. doi:S1535610803002411 [pii]. [PubMed: 14585354]
43. Brun J, et al. Identification of genetically modified Maraba virus as an oncolytic rhabdovirus. Mol Ther. 2010; 18:1440–1449. [PubMed: 20551913]
44. Le Boeuf F, et al. Synergistic interaction between oncolytic viruses augments tumour killing. Mol Ther. 2011; 18:888–895.
45. Lun X, et al. Efficacy and safety/toxicity study of recombinant vaccinia virus JX-594 in two immunocompetent animal models of glioma. Mol Ther. 2010; 18:1927–1936. [PubMed: 20808290]
46. Mikus J, Steverding D. A simple colorimetric method to screen drug cytotoxicity against Leishmania using the dye Alamar Blue. Parasitol Int. 2000; 48:265–269. [PubMed: 11227767]
47. Chou TC, Talaly P. A simple generalized equation for the analysis of multiple inhibitions of Michaelis-Menten kinetic systems. J Biol Chem. 1977; 252:6438–6442. [PubMed: 893418]

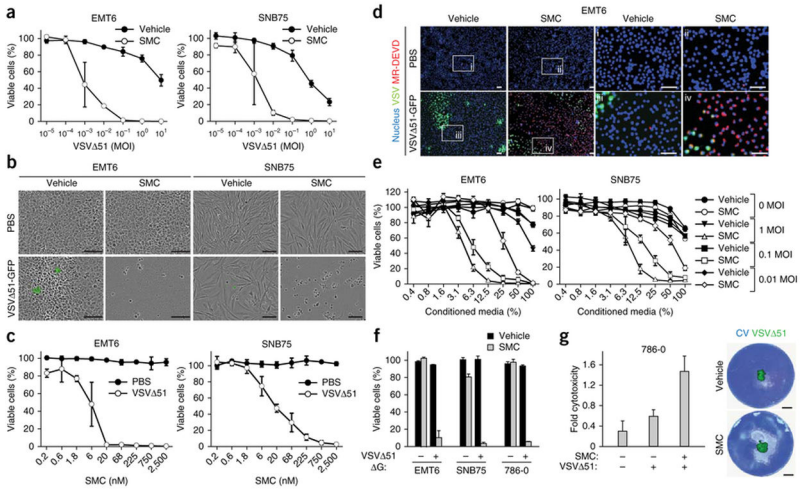

Figure 1. SMC synergizes with oncolytic rhabdoviruses to induce bystander death of cancer cells

a, Alamar blue viability assays of EMT6 and SNB75 cells treated with vehicle or 5 μM LCL161 and increasing multiplicity of infection (MOI) of VSVΔ51 for 48 hr. Error bars, mean ± s.d. n = 4. **b,** Micrographs of cells treated with vehicle or 5 μM LCL161 and PBS or 0.1 MOI of VSVΔ51-GFP. Scale bar, 100 μm. **c,** Alamar blue viability assays of cells infected with PBS or 0.1 MOI of VSVΔ51 (0.1 MOI) in the presence of increasing concentrations of LCL161 for 48 hr. Error bars, mean ± s.d. n = 3. **d,** Cells were stained with Hoechst (nucleus) and MR-DEVD (to reveal active caspase-3) cells after co-treatment with 5 μM LCL161 and 0.01 MOI of VSVΔ51-GFP for 36 hr. i–iv are higher magnification images of the boxed areas. Scale bar, 100 μm. **e,** Cells were infected with VSVΔ51 at the indicated MOI for 24 hr, cell culture supernatant was exposed to virus-inactivating UV light and then supernatant was applied at indicated dilutions to new cells in the presence of vehicle or 5 μM LCL161. Alamar blue viability assays were performed 48 hr post-treatment. Error bars, mean ± s.d. n = 3. **f,** Cells were cotreated with vehicle or 5 μM LCL161 and non-spreading virus VSVΔ51ΔG (0.1 MOI). Alamar blue viability assays were performed at 48 hr post-treatment. Error bars, mean ± s.d. n = 3. **g,** Cells were overlaid with agarose media containing 5 μM LCL161 and inoculated with 500 PFU of VSVΔ51-GFP in the middle of the well. At 96 hr post-treatment, virus infectivity was measured by fluorescence and cytotoxicity was assessed by crystal violet (CV) staining. Images were superimposed; non-superimposed images are in Supplementary Fig. 6. Error bars, mean ± s.d. n = 4. Scale bar, 5 mm. All figure panels: representative data from at least three independent experiments using biological replicates.

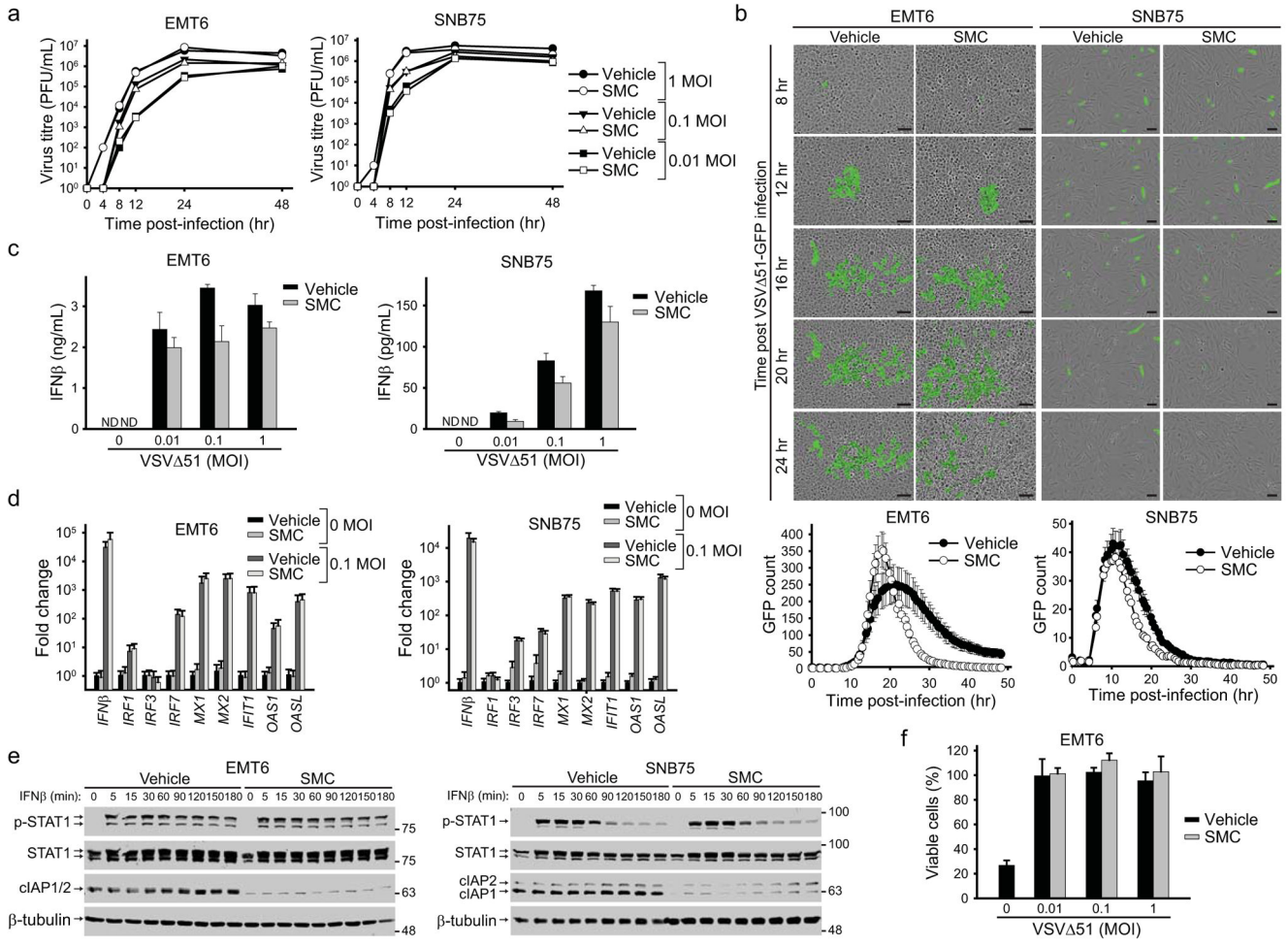

Figure 2. SMC treatment does not alter the antiviral response of cancer cells

a, Cells were pretreated with vehicle or 5 μM LCL161 for 2 hr and infected with the indicated MOI of VSVΔ51. At indicated time points, virus titre was assessed by a standard plaque assay. Error bars, mean ± s.d. **b,** Cells were treated with vehicle or 5 μM LCL161 and infected with VSVΔ51-GFP (0.1 MOI). Cells were imaged every 30 minutes using the Incucyte Zoom. Images are representative of four experiments and graphs below images show the number of GFP signals detected at each time point was plotted. Error bars, mean ± s.d. n = 12. Scale bar, 100 μm. **c,** Cell culture supernatants from cells treated with vehicle or 5 μM LCL161 and indicated MOI of VSVΔ51 for 24 hr were processed for the presence of IFNβ by ELISA. Error bars, mean ± s.d. n = 3. **d,** Cells were treated with vehicle or 5 μM LCL161 and indicated MOI of VSVΔ51 for 20 hr. Cells were then processed for RT-qPCR to measure expression of virus and IFN stimulated gene transcripts indicated on the x-axis. Error bars, mean ± s.d. n = 3. **e,** Cells were pretreated with 5 μM LCL161 for 2 hr and subsequently stimulated with IFNβ for the indicated times. Total and phosphorylated STAT1 was measured by Western blot. **f,** EMT6 cells were treated with vehicle or 5 μM LCL161 and infected with the indicated MOI of VSVΔ51 for 20 hr. Media was exposed to UV light and then applied to uninfected cells. Cells were subsequently challenged with 1 MOI of wild-type VSV for 48 hr and the proportion of rescue of cell death from wild-type VSV was

measured by an Alamar Blue viability assay. Error bars, mean ± s.d. n = 3. All figure panels: representative data from at least three independent experiments using biological replicates.

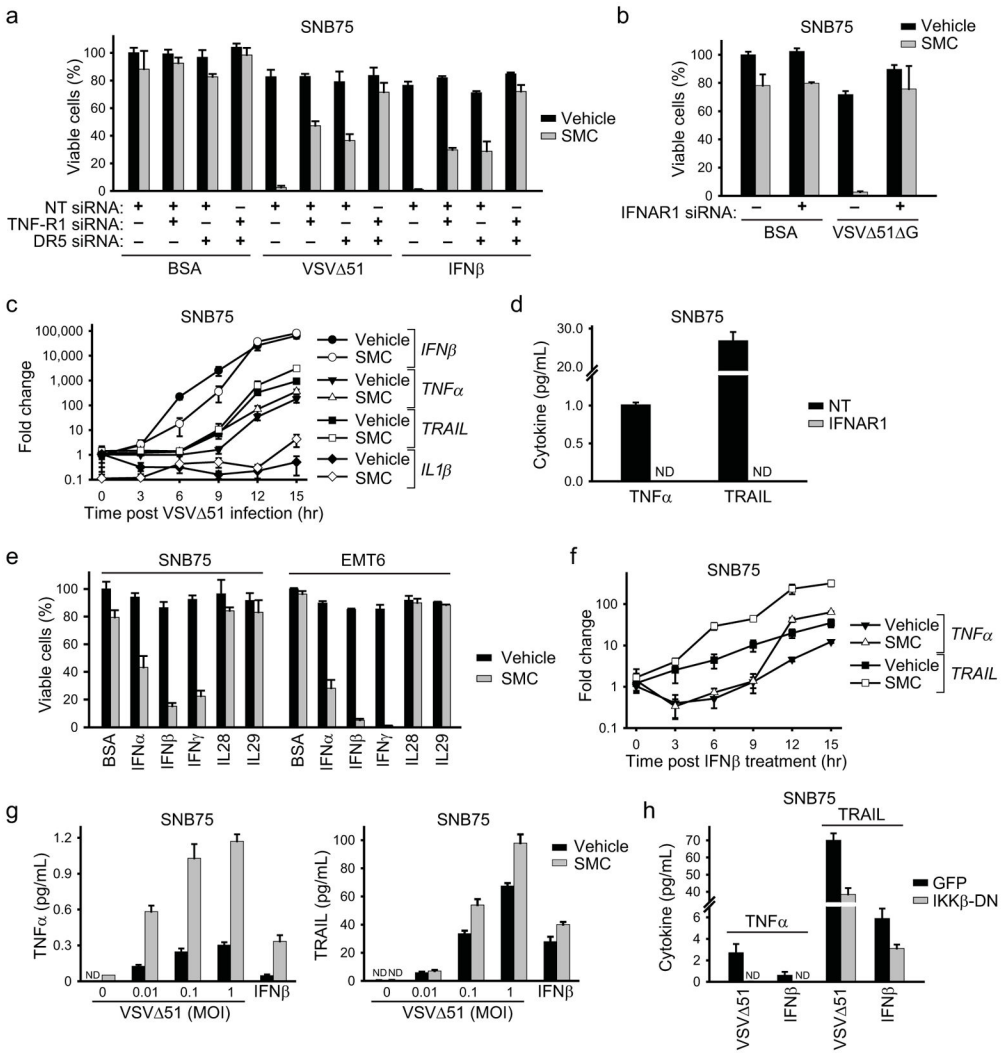

Figure 3. Roles for type 1 IFN- and NF-κB-dependent proinflammatory cytokines

a, Alamar blue viability assay of cells transfected with combinations of nontargeting (NT), TNF-R1 and DR5 siRNA for 48 hr and subsequently treated with vehicle or 5 μM LCL161 and with BSA (control), 0.1 MOI VSVΔ51 or 250 U/mL IFNβ for 48 hr. Error bars, mean ± s.d. **b,** Alamar blue viability assay of cells transfected with NT or IFNAR1 siRNA for 48 hr and subsequently treated with vehicle or 5 μM LCL161 and with BSA (control) or 0.1 MOI VSVΔ51ΔG for 48 hr. Error bars, mean ± s.d. **c,** Cells were pretreated with vehicle or 5 μM LCL161 for 2 hr, infected with 0.5 MOI VSVΔ51, and expression of transcripts encoding the indicated cytokines was measured by RT-qPCR at the indicated times. Error bars, mean ± s.d. **d,** Cells were transfected with NT or IFNAR1 siRNA for 48 hr and subsequently treated with LCL161 and 0.1 MOI VSVΔ51 for 24 hr. TNFα and TRAIL in supernatants were measured by ELISA. Error bars, mean ± s.d. **e,** Alamar blue viability assay of cells treated with vehicle or 5 μM LCL161 together with cytokines indicated on the x-axis (BSA, control) for 48 hr. Error bars, mean ± s.d. **f,** Cells were pretreated with LCL161, stimulated with 250 U/mL (~20 pg/mL) IFNβ and TRAIL and TNFα mRNA levels were determined by RT-qPCR at the indicated time points. Error bars, mean ± s.d. **g,** Cells were treated with

vehicle or 5 μM LCL161 and the indicated MOI VSVΔ51 or 250 U/mL IFNβ for 24 hr. TNFα and TRAIL in supernatants were measured by ELISA. **h,** Cells expressing GFP (control) IKKβ-DN were treated with 5 μM LCL161 and 0.1 MOI VSVΔ51 or 250 U/mL IFNβ for 24 hr. TNFα and TRAIL in supernatants were measured by ELISA. Error bars, mean ± s.d. All figure panels: representative data from at least three independent experiments using biological replicates (n = 3).

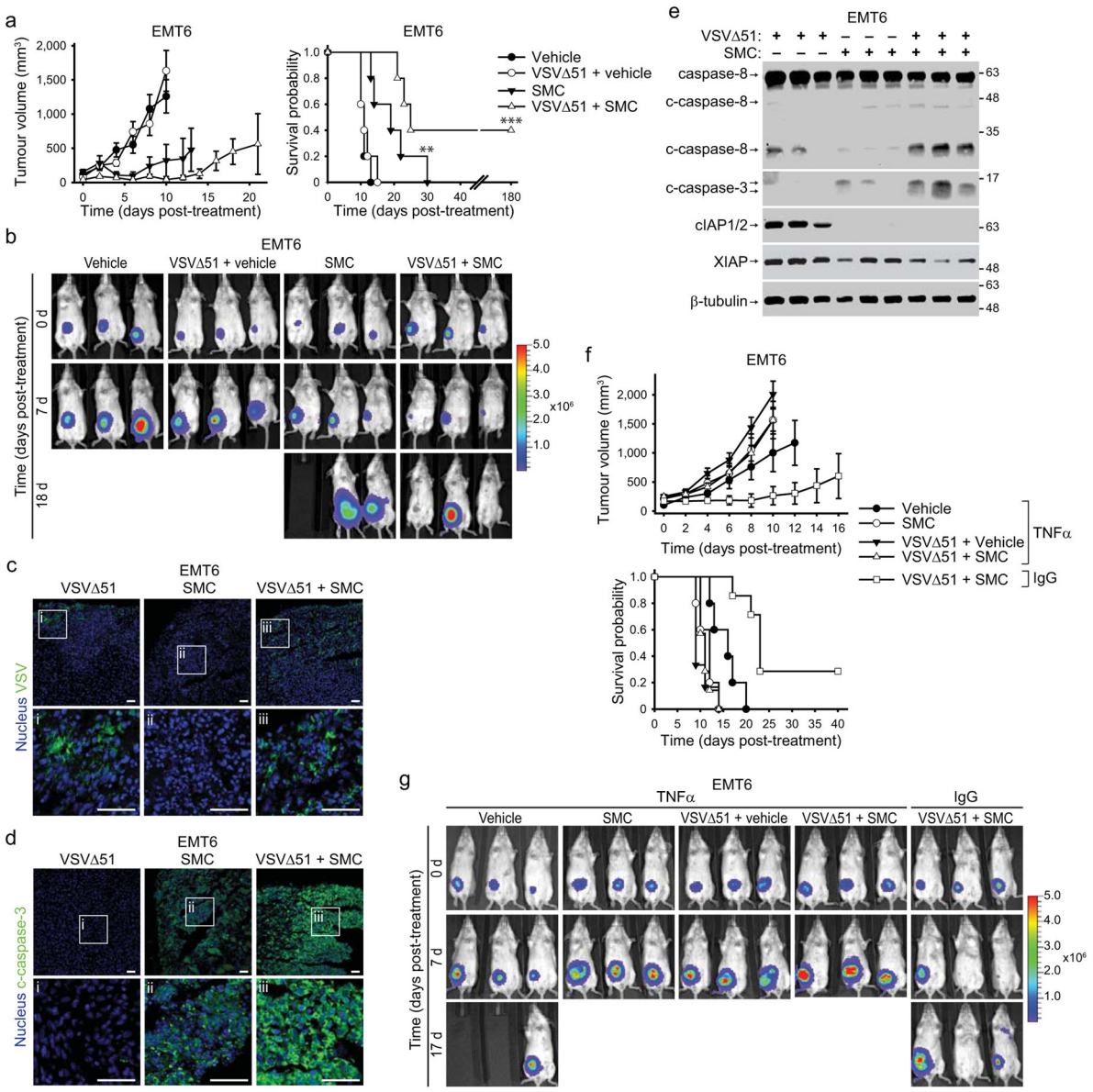

Figure 4. Combinatorial SMC and OV treatment is efficacious *in vivo* and depends on cytokine signalling

a, Mice bearing ~100mm^3 EMT6-Fluc tumors were treated with vehicle or with 50 mg/kg LCL161 (oral) and/or 5×10^8 PFU VSVΔ51 (i.v.). Left panel depicts tumour growth. Right panel represents the Kaplan-Meier curve depicting mouse survival. Error bars, mean ± s.e.m. n = 5 per group. Log-rank with Holm-Sidak multiple comparison: **, $p < 0.01$; ***, $p < 0.001$. Representative data from two independent experiments. **b,** Representative IVIS images from mice described in (a) were acquired at indicated time points. Scale: p/sec/cm^2/sr. **c, d,** 24h after treatment as in (a), tumors were isolated and analyzed by immunofluorescence using VSV (c) or c-caspase-3-specific (d) antibodies. i–iii are higher magnification images of the boxed areas in the top row. Scale bar, 50 μm**.** Representative data from two experiments. **e,** Lysates of tumors from mice treated for 20 hr as in (a) were

blotted with the indicated antibodies. Representative data from two experiments. **f,** Mice bearing ~100mm^3 EMT6-Fluc tumors were treated with neutralising TNFα antibody or isotype control (IgG) antibody, and subsequently treated with 50 mg/kg LCL161 (oral) and/or 5×10^8 PFU VSVΔ51 (i.v.). Top panel depicts tumor growth. Bottom panel represents the Kaplan-Meier curve depicting mouse survival. Error bars, mean ± s.e.m. Vehicle α-TNFα, n = 5; SMC α-TNFα, n= 5; vehicle+VSVΔ51, n=5; α-TNFα, n = 5; SMC+VSVΔ51 α-TNFα, n = 7; SMC+VSVΔ51 α-IgG, n = 7. Log-rank with Holm-Sidak multiple comparison: ***, $p < 0.001$. **g,** Representative IVIS images from mice from (f). Scale: p/sec/cm^2/sr.

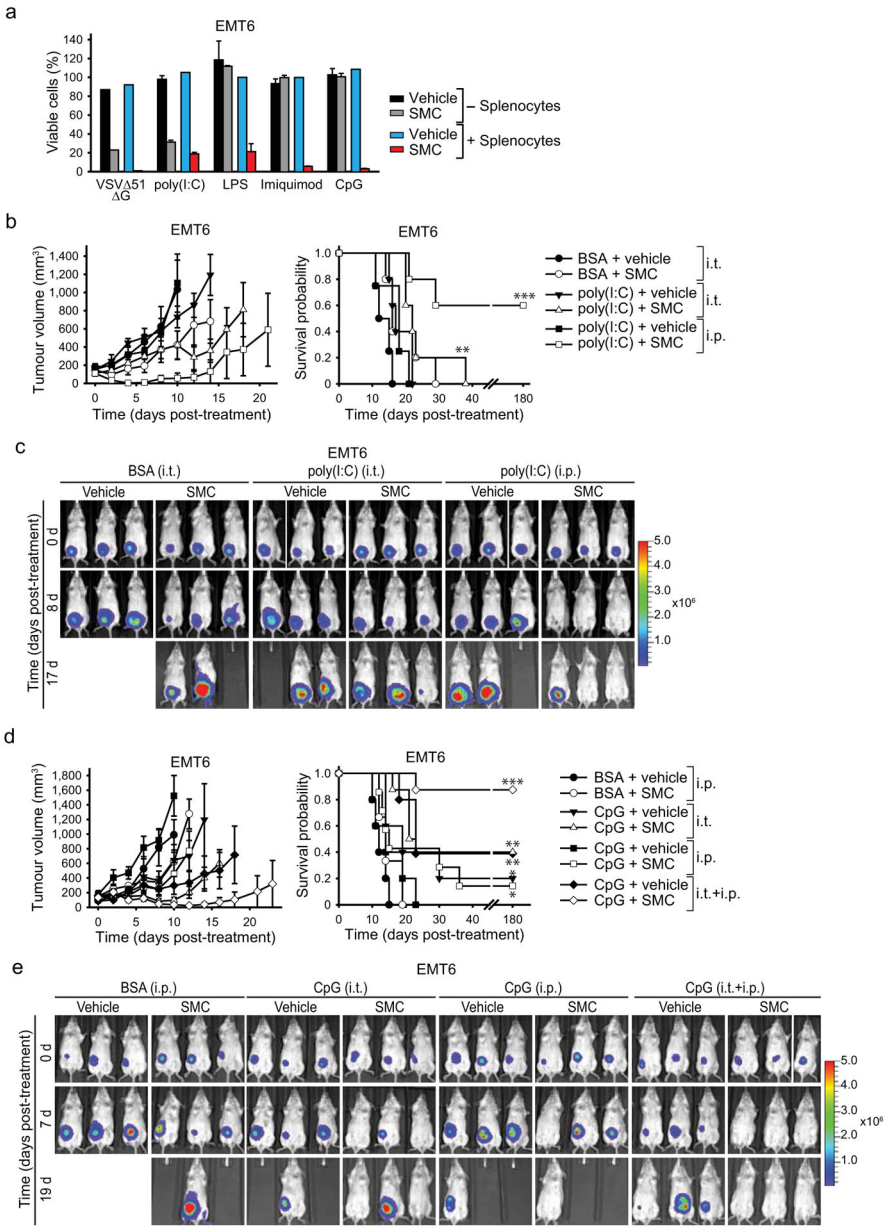

Figure 5. Adjuvants synergize with SMC therapy in murine cancer models

a, Alamar blue viability assays of EMT6 cells which were cocultured or not with splenocytes in a transwell system, and for which the segregated splenocytes were treated with vehicle or 1 μM LCL161 and 0.1 MOI VSVΔ51ΔG (positive control) or the indicated TLR agonists (1 ug/mL poly(I:C) (TLR3); 1 ug/mL LPS (TLR4), 2 μM imiquimod (TLR7), 0.25 μM CpG (TLR9)) for 24 hr. Error bars, mean ± s.d. Representative data from three independent experiments using biological replicates (n = 3). **b,** Mice with established EMT6-Fluc tumors (~100mm^3) were treated with LCL161 (50 mg/kg LCL161, oral) and poly(I:C) (15 ug intratumoral (i.t.). or 2.5 mg/kg i.p.). Left panel depicts tumour growth. Right panel represents the Kaplan-Meier curve depicting mouse survival. Vehicle, vehicle +poly(I:C) i.p., n = 4; remaining groups, n = 5.. Error bars, mean ± s.e.m. Log-rank with

Holm-Sidak multiple comparison: **, $p < 0.01$; ***, $p < 0.001$. **c,** Representative IVIS images from mice treated in (b). Scale: p/sec/cm^2/sr. **d,** Mice with established EMT6-Fluc tumors (~100mm^3) were treated with 50 mg/kg LCL161 (oral) alone or in combination with 200 μg (i.t.) and/or 2.5 mg/kg (i.p.) CpG ODN 2216. Left panel depicts tumor growth. Right panel represents the Kaplan-Meier curve depicting mouse survival. Vehicle, n = 5; SMC, n= 5; vehicle+CpG i.p., n = 5; SMC+CpG i.p., n = 7; vehicle+CpG i.t., n = 5; SMC+CpG i.t., n = 8; vehicle+CpG i.p.+i.t., n = 5; SMC+CpG i.p.+i.t., n = 8. Error bars, mean ± s.e.m. Log-rank with Holm-Sidak multiple comparison: *, $p < 0.05$; **, $p < 0.01$; ***, $p < 0.001$. **e,** Representative IVIS images from mice treated as in (d). Scale: p/sec/cm^2/sr.